Optimal Search Strategy

——A generic model of plane searching

Table of Contents

1. Introduction 2
1.1 Background knowledge 2
1.2 Existing search strategy 2
1.2.1 Search equipment 2
1.2.2 Search patterns 3
2. Problem Analysis 5
2.1 Goals 5
2.2 The Layout of Problem Solving 5
3. General Assumptions 6
4. Model Design and Solving 7
4.1 Model 1--- Airline 7
4.2 Model 2--- Projectile motion 8
4.3 Model 3--- The disturbance of wind and ocean current 11
4.3.1 Floating Process 11
4.3.2 Sinking Process 14
4.4 Model 4--- Search pattern 16
4.4.1 Model of radar or sonar system 17
4.4.2 Sector search pattern 17
4.4.3 Expanding square search pattern 19
4.4.4 Estimate effectiveness and efficiency 20
4.4.5 Comparison between two search patterns 21
5. Verifications of our model 23
5.1 Verification of Model 1 23
5.2 Verification of Model 2 23
6. Sensitivity Analysis 24
7. Weaknesses and Strengths of the Model 27
8. References 29
9. Appendix (Non-technical Paper) 30

1. Introduction

1.1 Background knowledge

At 17:22 UTC on 7th March 2014 Malaysian Airlines flight MH370 carrying 239 passenger and crew from Kuala Lumpur to Beijing lost contact with Air Traffic Control and was subsequently reported missed. Neither the crew nor the aircraft's communication systems relayed a distress signal, indications of bad weather or technical problems before the aircraft vanished. Malaysia established the Joint Investigation Team (JIT) to investigate the incident, working with foreign aviation authorities and experts. Nevertheless, the extensive air and sea search was made around the last reported location of the aircraft without success [1].

1.2 Existing search strategy

The critical principle of existing search strategies is to determine the datum-mark and baseline according to Last Known Positions (LKPs) and related location reports. Hence searchers can determine main air and sea search area in accordance to the calculation of the influence of sea wind and ocean currents. The datum-mark is defined as the point where airplane plunge into water [2].

1.2.1 Search equipment



Seaplane



Helicopter



Maritime surveillance aircraft



Search Vessel



Bluefin-21 Autonomous Underwater Vehicle



Iridium Self Locating Datum Marker Buoy

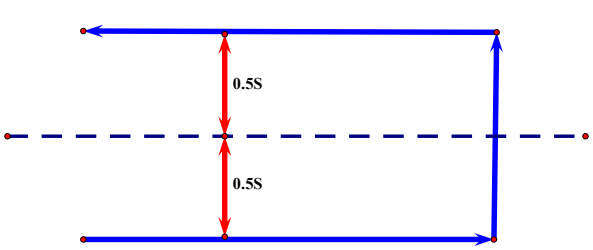
Fig.1.2.1 Different searching equipment

The search planes and vessels use sonar, radar system and infrared, long-range and high resolution cameras - plus their own eyesight - to search the ocean. They also film everything so they can review what they've seen after they return to base.

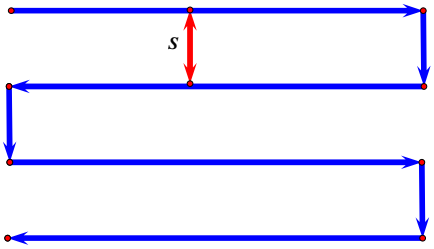
The buoys resemble a poster tube, each about 1 meter (3.3 feet) long, with an antenna that transmits a GPS signal that can be tracked by searchers. The idea is that the buoys drift in a manner similar to any debris, giving searchers clues as to where debris might move over time. However, the wind can move the buoys at a different rate with floating debris — but usually we do not take the difference into consideration.

1.2.2 Search patterns

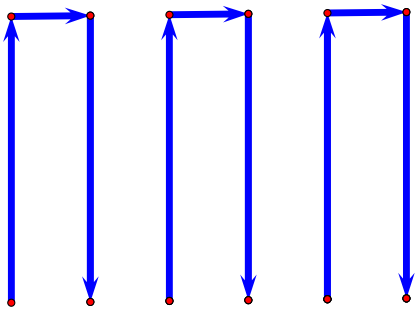
Search patterns are the planned routes for vessels or planes to search the most possible areas of debris. A suitable search pattern determines the speed and success of a search task. Some common search patterns include track line search pattern, parallel sweep search pattern, coordinated creep line search pattern, sector search pattern and expanding square search [3].



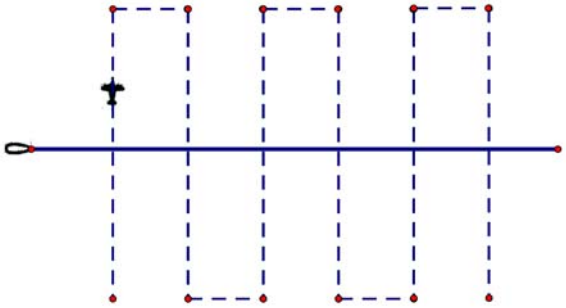
Track line search pattern



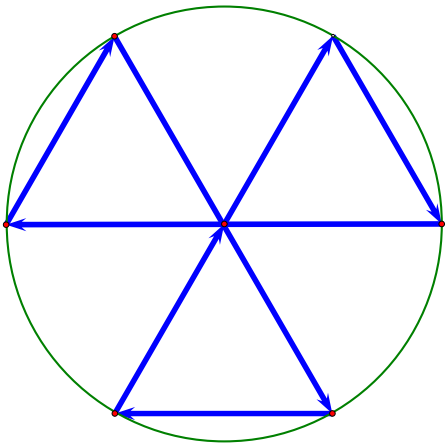
Parallel sweep search pattern for a single ship



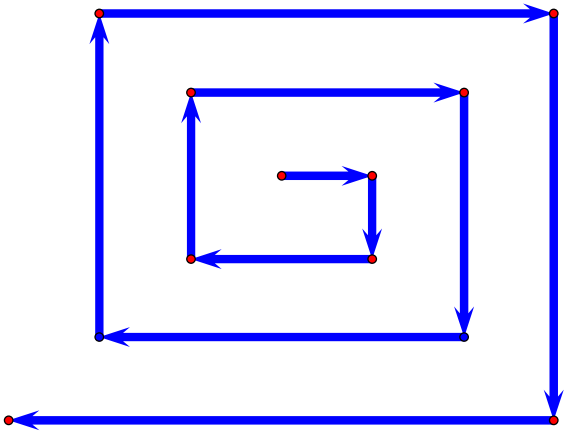
Parallel sweep search pattern for 3 vessels



Coordinated creep line search pattern



Sector search pattern



Expanding square search pattern

Fig1.2.2 Different search patterns

Track line search pattern searches along the track line, which is fast and effective if survivors are in nearby area. Parallel sweep search pattern searches equably in a large area along the prospective direction and it can be operated with multiple vessels simultaneously. Coordinated creep line search is applied when both aircraft and vessels are available. When search target is located in a limited area, sector search pattern is effective. Buoys with GPS are used to set as the datum-mark. Expanding square search pattern searches from the datum-mark and expands search lines outward.

2. Problem Analysis

2.1 Goals

In order to construct a generic mathematical model that could assist in searching, we divide the solution into four steps:

- Determine the optimal airline and possible losing-contact point between given location A and B.
- Compute the probable datum-mark using projectile motion model.
- Delimit possible search area considering ocean and wind current.
- Compare different search patterns and select optimal search strategy.

2.2 The Layout of Problem Solving

Based on the given longitude and latitude of departure A and destination B, we construct a 3-dimensional Cartesian coordinate system having its origin at the center of the earth. The plane is assumed to sail through the great-circle course [4]. We figure out the function of the airline and determine the accurate lost-contact point of the airline.

The plane is assumed to perform the projectile motion after losing contact. Generic equations of projectile motion considering earth rotation and air resistance have been constructed and analytically solved in Model 2. Datum-mark can be found by solving the above equations

FVCOM model [5] and reformulated Navier-Stokes equations [6] have been applied to analyze the impact ocean and wind currents performing on the plane wreckages. The floating process is assumed to be discrete and be a Markov Chain [7]. We build a model to further figure out the final position, using differential equation to describe the floating process, in which we reasonably assume the wind velocity obeys logarithmic normal distribution [8]. For those wreckages which have high density, we develop an independent model to calculate the location coordinate where wreckages sink.

We select two common searching patterns, which are sector search pattern and expanding square search pattern, and define three indexes to evaluate their efficiency and effectiveness. Lagrange-Galerkin method [6] and Monte Carlo Method [9] are applied in Model 4 in order to simulate the searching strategy. Through comparison, we have concluded that under different conditions (such as wind velocity), sector search pattern and expanding square search pattern have different effectiveness and efficiency, and also have pointed out their significant weaknesses.

3. General Assumptions

We generally make the following assumptions in this paper:

- Assuming the earth is a strict sphere.
- Assuming that plane would fly strictly along the great circle course instead of rhumb lines in order to shorten flying distance.
- Assuming that the plane begins to fall down at the moment when the plane loses contact.
- Assuming the plane is a particle in all models (ignoring its size and volume).
- Assuming that the falling process obeys the law of projectile motion (considering air resistance and earth rotation)
- Assuming that the floating process of aircraft wreckage is discrete and obeys the law of Markov process.
- Assuming the velocity of sea wind obeys the normal logarithmic distribution.
- Assuming the sea level and seabed (in Model 3) are strict geometric planes (without depth changes).

Table 1.
Notation.

Symbol	Meaning
R	**The earth radius**
P	**The point where plane loses contact**
ω	**Rotation angle of earth**
k	**Resistance constant**
v	**Given velocity when the plane begins to fall**
h	**Height of projectile motion**
2α	**Top angle of the cross section triangle from the cone shape scan area**
H	**The flying height of a search plane**
t_0	**Time from the aircraft crashed on ocean surface till rescue team arrived and set up the buoy**

Symbol	Meaning
λ	**Latitude of the plane**
v_0	Initial velocity of projectile motion
f	**Drag force of projectile motion**
μ	Average number of wind velocity
σ^2	**Variance of wind velocity**
s	The distance of the target to the point directly below of the search plane
$p(s)$	**Possibility of finding the target for a radar or sonar system**
T	Location of target
PS	**The total possibility of target being found by multiple routes**
TS	Expectation time of finding the target (if target could be found)
$l(x,y)$	**Possibility of target falling to the point (x,y)**
t_i	Flight time to find target on route i
R_m	**Maximum possible value of floating radius**
E	**Expectation of the possibility of finding the target per time**

4. Model Design and Solving

4.1 Model 1--- Airline

To work out the function of great-circle airline [4], let **x**, **y**, **z** be three rectangular coordinates having their origin at the center of the earth, **z** corresponding with the axis (pointing at the North Pole), **x** through prime meridian. A and B are two given points which respectively represent the departure and destination (The figure shows the case where A lies on the prime meridian. Actually, the location of A is random and does not affect the effectiveness of the final equation.)

Since flying height is approximately 0.1% of earth radius R, we ignore the flying height when locating the plane. Simply denote the coordinates of A and B as (p_1, q_1) and (p_2, q_2) in longitude-latitude coordinate system, (x_1, y_1, z_1) and (x_2, y_2, z_2) in 3-dimensional rectangular coordinate system.

Denote the point where the plane lost contact as P. The fundamental problem is to work out the coordinate of P.

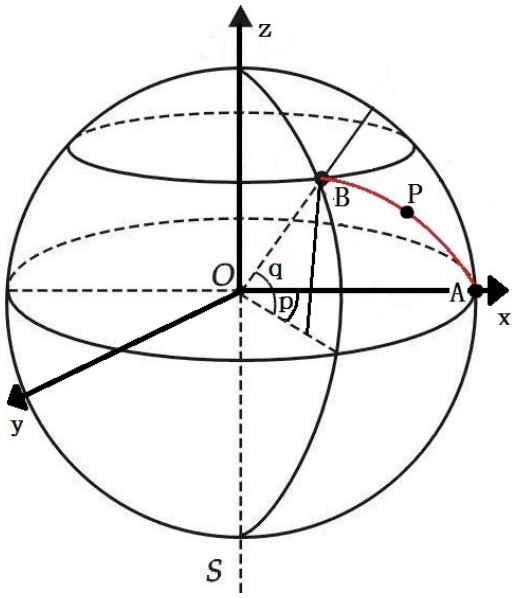


Fig 4.1.1 Great Circle Course

First, the longitude- latitude coordinate given needs conversion into rectangular coordinate. Work out the coordinate conversion formula.

$$\begin{cases} x = \mathrm{R}\cos(p)\cos(q) \\ y = \mathrm{R}\sin(p)\cos(q) \\ z = Rsin(q) \end{cases}$$

As is defined above, the airline is simply the great arc (a segment of the great circle determined by O, A, B) between A and B which has a central angle smaller than 180°.

Respectively denote the arc length and the chord length between A and P as *s* and *d*. s represents the distance plane already flew. The relationship between s and d is given in equation below.

$$d = 2\mathrm{R}\sin\frac{s}{2R}$$

The great circle can be recognized as intersects of plane OAB and spherical surface. The function of plane OAB can be solved with knowledge of 3-dimensional analytic geometry (Equation (4.1.1)).

$$\begin{aligned}&[R^2\sin(p_2)\sin(q_1)\cos(q_2) - R^2\sin(p_1)\cos(q_1)\sin(q_2)]x\\ &+ [R^2\cos(p_1)\cos(q_1)\sin(q_2) - R^2\cos(p_2)\sin(q_1)\cos(q_2)]y\\ &+ [R^2\cos(p_1)\sin(p_2)\cos(q_1)\cos(q_2) - R^2\sin(p_1)\cos(p_2)\cos(q_1)\sin(q_2)]z = 0\end{aligned} \tag{4.1.1}$$

Equation (4.1.a) gives the function of the sphere with point A as its center and d as its radius.

Through observation of the figure 4.1.1, P can be recognized as intersect of spherical sphere O, plane OAB and the spherical sphere determined by equation (4.1.a). Hence, we have the following equations, whose solution is the coordinate of P.

$$\begin{cases} x^2 + y^2 + z^2 = R^2 \\ (x - Rcos(p_1)cos(q_1))^2 + (y - Rsin(p_1)\cos(q_1))^2 + \left(z - Rsin(\mathrm{q}_1)\right)^2 = 4R^2\sin^2\left(\frac{S}{2R}\right) \end{cases} \tag{4.1.a}$$

(4.1.1)

(4.1.2)

The longitude-latitude coordinate is expected in the final result. Hence, we provide the following conversion formula from rectangular coordinate to longitude-latitude coordinate.

$$\begin{cases} p = \arctan(\frac{y}{x}) \\ q = \arcsin(\frac{z}{R}) \end{cases}$$

Denote the final result as$\left(p_{P,}q_P\right)$. After getting this coordinate, combined with the given height information, we can apply the data above in the projectile motion equations in Model 2 to work out the accurate plunging point, which is fundamental to determine the datum-mark.

The Verification Part in this paper cites the example of Air France Flight 477 and supports the effectiveness of this model.

4.2 Model 2--- Projectile motion

As we have assumed above, the plane begins to fall down at the moment when the plane loses contact, the plane is a particle when falling and the falling process obeys the law of projectile motion [10].

In this model, the appropriate drag force relation and Coriolis force are incorporated into the equations of projectile motion. Under these conditions, an exact time-explicit solution to the equations can be obtained.

Let the earth (seen as a sphere) be the reference system.

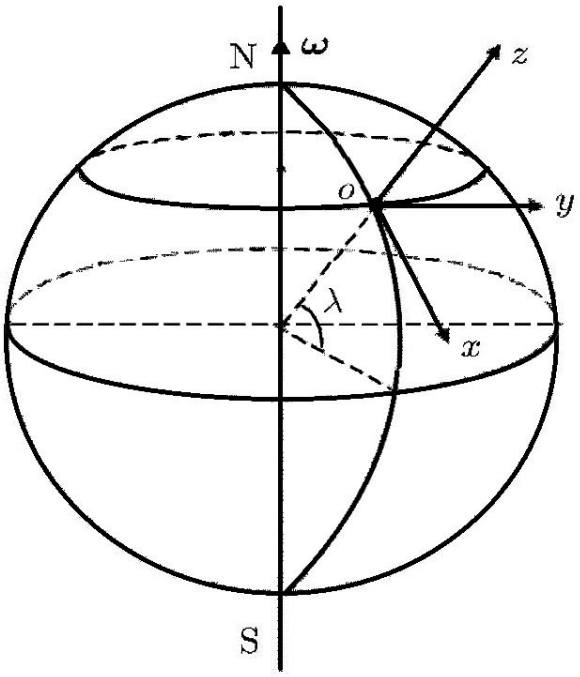


Fig 4.2.1 Earth with rectangular coordinate system

Construct a fixed coordinate system OXYZ, orienting from O of the earth surface, at which the latitude is λ (seen as Figure 1). OX is southwardly tangent to the meridian, OY is eastwardly tangent to the parallel, OZ is upwardly perpendicular to the ground. Rotation angle ω moves on the axis of the earth SN, where $\boldsymbol{\omega} = -\boldsymbol{i}\omega\cos\lambda + \boldsymbol{k}\omega\sin\lambda$. In most applications, we approximately take ω = 7.3 ×10−5rad/s (derive from the fact that the earth goes through one complete rotation in 24 hours).

Denote the mass of object as m and initial velocity of $\boldsymbol{v_0}$ is projected in any direction from O. In order to simplify the problem， the drag force is typically modeled as proportional to the projectile speed (the linear drag model) f = −mkv， and k is resistance constant. So object motion equations can be obtained as follows (from Newton Second Law):

$$m\ddot{x} = 2m\omega\dot{y}\sin\lambda - mk\dot{x} \tag{4.2.1a}$$

$$m\ddot{y} = -2m\omega(\dot{x}\sin\lambda + \dot{z}\cos\lambda) - mk\dot{y} \tag{4.2.1b}$$

$$m\ddot{z} = 2m\omega\ddot{y}\cos\lambda - mk\dot{z} - mg \tag{4.2.1c}$$

The initial conditions are given：

when t = 0 , x = y = z = 0,

$$\dot{x} = v_0 \cos\alpha,$$

$$\dot{y} = v_0 \cos\beta,$$

$$\dot{z} = v_0 \cos\gamma,$$

where $\cos 2\alpha + \cos 2\beta + \cos 2\gamma = 1$

We integrate (1a) (1b) and (1c), thus having:

$$\dot{x} = 2\omega y \sin\lambda - kx + v_0 \cos\alpha \tag{4.2.2a}$$

$$\dot{y} = -2\omega(x \sin\lambda + z \cos\lambda) - ky + v_0 \cos\beta \tag{4.2.2b}$$

$$\dot{z} = 2\omega y \cos\lambda - kz - gt + v_0 \cos\gamma \tag{4.2.2c}$$

According to (1b) (2a) (2b) and (2c), then we have:

$$\ddot{y} + 2k\dot{y} + (k^2 + 4\omega^2)y = 2\omega gt \cos\lambda - 2\omega \boldsymbol{v_0} \cos\alpha \sin\lambda - 2\omega \boldsymbol{v_0} \cos\gamma \cos\lambda + k\boldsymbol{v_0} \cos\beta$$

So we can find the solution:

$$y = e^{-kt}(c_1 \cos 2\omega t + c_2 \sin 2\omega t) + \frac{2g\omega \cos\lambda}{k^2+4\omega^2} t + \left(q - \frac{4gk\omega \cos\lambda}{k^2+4\omega^2}\right)$$

Where $q = k\boldsymbol{v_0} \cos\beta - 2\omega \boldsymbol{v_0} \cos\alpha \sin\lambda - 2\omega \boldsymbol{v_0} \cos\gamma \cos\lambda$

(4.2.3)

Using the initial value, we get:

$$c_1 = \left(\frac{4gk\omega \cos\lambda}{k^2 + 4\omega^2} - q\right)/(k^2 + 4\omega^2)$$

$$c_2 = \frac{1}{2\omega}\left[v_0 \cos\beta + \left(\frac{4gk\omega \cos\lambda}{k^2 + 4\omega^2} - q\right)/(k^2 + 4\omega^2) - \frac{2g\omega \cos\lambda}{k^2 + 4\omega^2}\right]$$

According to (2a), (2c) and (3), then we have:

$$\begin{aligned} x = \Bigg[& c_1 \sin\lambda \sin 2\omega t - c_2 \sin\lambda \cos 2\omega t + \frac{4\,\omega^2 g \sin\lambda \cos\lambda}{k^2 + 4\omega^2}\left(\frac{te^{kt}}{k} - \frac{e^{kt}}{k^2}\right) \\ & + \frac{2\omega \sin\lambda}{k(k^2 + 4\omega^2)}\left(q - \frac{4gk\omega \cos\lambda}{k^2 + 4\omega^2}\right)\left(e^{kt} - 1\right) + \frac{v_0}{k}\cos\alpha\left(e^{kt} - 1\right) + c_2 \sin\lambda \\ & + \frac{1}{k^2} \cdot \frac{4\,\omega^2 g \sin\lambda \cos\lambda}{k^2 + 4\omega^2}\Bigg] e^{-kt} \end{aligned} \tag{4.2.4}$$

$$z = \left[c_1 \cos\lambda \sin 2\omega t - c_2 \cos\lambda \cos 2\omega t + \frac{4\,\omega^2 g \cos^2\lambda}{k^2 + 4\omega^2}\left(\frac{te^{kt}}{k} - \frac{e^{kt}}{k^2}\right) + \frac{2\omega \cos\lambda}{k(k^2 + 4\omega^2)}\left(q - \frac{4gk\omega \cos\lambda}{k^2 + 4\omega^2}\right)\left(e^{-kt} - 1\right) - g\left(\frac{te^{kt}}{k} - \frac{e^{kt}}{k^2}\right) + \frac{v_0}{k}\cos\gamma\left(e^{-kt} - 1\right) + c_2 \cos\lambda + \frac{1}{k^2} \cdot \frac{4\,\omega^2 g \cos^2\lambda}{k^2 + 4\omega^2} - \frac{g}{k^2}\right] e^{-kt} \tag{4.2.5}$$

Above all, (3), (4) and (5) give the exact time-explicit solutions considering the earth rotation and air resistance to the equations.

In (3), (4) and (5), v_0 is the initial velocity of projectile motion. Since v is the given velocity when the plane begins to fall, according to Conservation of Energy Theorem, we have:

$$\frac{1}{2} m {v_0}^2 = \frac{1}{2} m v^2 + mg\mathrm{h}$$

Here, in order to simplify the calculation, we assume that the falling plane wouldn't be influenced by the earth rotation and air resistance.

Obviously, $v_0 = \sqrt[2]{v^2 + 2g\mathrm{h}}$

Now we determine the plunging point (x, y, z)

In this model, we simply let z=0 be the plunging condition to simplify the calculation. Apparently, the plane z=0 is the tangent plane of the earth spherical surface. When the initial velocity and lasting time are not significant, the horizontal displacement is also negligible compared to the huge earth radius. Thus using condition z=0 can get a relatively accurate result. Actually, the cruise speed of an ordinary civil airplane is about 800km/h (222m/s) and the flying height is approximately 9000m. The horizontal range is approximate 10000m (10km), which is only 0.2% of the earth radius.

Hence, let equation (5) equal 0. The solution gives the value of t. Denote the solution as t_0.

Let t equal t_0 and v_0 equal $\sqrt[2]{v^2 + 2g\mathrm{h}}$ (in equation (3), (4), (5)). Now we get the coordinate of the plunging point.

The plunging point is fundamental for rescuers to determine a probable searching area. However, after plunging into water, the location of wreckage is affected greatly by the ocean current and wind velocity. Therefore, Model 3 specifically discusses these effects in order to further delimit the searching area.

4.3 Model 3--- The disturbance of wind and ocean current

4.3.1 Floating Process

A floating object will be motivated by the surrounding water and its velocity will be changed by the water speed. We apply the Unstructured Grid Finite Volume Community Ocean Model (FVCOM) [7] and the Navier-Stokes equations [6] to analyze the surface flow field. FVCOM model is a prognostic,

unstructured-grid, finite-volume, free-surface, 3-D primitive equation coastal ocean circulation model developed by UMASSD-WHOI joint efforts [7]. The Primitive Equations governing the ocean model for the flow velocity are a reformulation of the three-dimensional Navier-Stokes equations under the Boussinesq and hydrostatic approximations [6].

Momentum and continuity equations are given below:

$$\frac{\partial u}{\partial t}+u\frac{\partial u}{\partial x}+v\frac{\partial v}{\partial y}+w\frac{\partial u}{\partial z}-fv+\frac{1}{\rho_0}\frac{\partial p}{\partial x}=v_H\left(\frac{\partial^2 u}{\partial x^2}+\frac{\partial^2 u}{\partial y^2}\right)+v_z\frac{\partial^2 u}{\partial z^2} \tag{4.3.1.1}$$

$$\frac{\partial v}{\partial t}+u\frac{\partial v}{\partial x}+v\frac{\partial v}{\partial y}+w\frac{\partial v}{\partial z}-fu+\frac{1}{\rho_0}\frac{\partial p}{\partial y}=v_H\left(\frac{\partial^2 v}{\partial x^2}+\frac{\partial^2 v}{\partial y^2}\right)+v_z\frac{\partial^2 v}{\partial z^2} \tag{4.3.1.2}$$

$$\int_{-H}^{0}(\frac{\partial u}{\partial x}+\frac{\partial v}{\partial y})dz=0, w(\boldsymbol{u})(x,y,z,t)=\int_{z}^{0}(\frac{\partial u}{\partial x}+\frac{\partial v}{\partial y})dz \tag{4.3.1.3}$$

Conservation equations for temperature θ_1 and salinity θ_2 are demonstrated below:

$$\frac{\partial \theta_i}{\partial t}+u\frac{\partial \theta_i}{\partial x}+v\frac{\partial \theta_i}{\partial y}+w\frac{\partial \theta_i}{\partial z}=A_i\left(\frac{\partial^2 \theta_i}{\partial x^2}+\frac{\partial^2 \theta_i}{\partial y^2}\right)+k_i\frac{\partial^2 \theta_i}{\partial z^2}\ ,i=1,2$$

$$p(x,y,z,t)=p_s(x,y,t)+g\int_{z}^{0}\rho(\theta_i,z')dz'$$

Where (u,v,w) is the three-dimensional velocity vector under the coordinate system (O, x, y, z).

ρ_0 is a constant reference density, g being the modulus of the acceleration of gravity and p_s the surface pressure. Further, $(-fv,fu)$ denote the components of the Coriolis force due to the rotation of the Earth. The coefficients $v_H\ and\ v_z$ denote the horizontal and vertical eddy viscosity coefficients for the horizontal velocity.

We can use second-order Runge-Kutta method to solve the above equations, but the calculation contains great uncertainy and many inaccurate facts, leading to greater deviation from the real floating trace as time goes on. So we introduce Lagrange-Galerkin method [6] and Monte Carlo method [9]. Also, in order to simplify calculation, we ignore temperature, salinity and density impact to the above problem.

Till now, the main difficulties of equations (1) to (3) are nonlinear convection terms and the non-local character of the divergence constraint. Here we propose, in the framework of finite elements, a modified Lagrange-Galerkin method introduced to integrate the nonlinear convection terms, combined with a fractional step projection method to deal with the divergence constraint. Let

$$\frac{dA}{dt}=\frac{\partial A}{\partial t}+u\frac{\partial A}{\partial x}+v\frac{\partial A}{\partial y}+w\frac{\partial A}{\partial z}$$

be the total derivative of A, where we let A be the velocity vector. The Lagrange-Galerkin method approximates $\frac{dA}{dt}$ at time instant t_{n+1} by the formula

$$\frac{dA(\boldsymbol{x},t)}{dt}|_{t=t_{n+1}} \approx \frac{A(\boldsymbol{x},t_{n+1}) - A(\boldsymbol{X}(\boldsymbol{x},t_{n+1};t_n),t_n)}{\Delta t}$$

(4.3.1.4)

Where $\boldsymbol{X}(\boldsymbol{x},t_{n+1};t_n)$ denotes the position at time t_n of a particle that, moving with the flow velocity $(\boldsymbol{u},\boldsymbol{v},\boldsymbol{w})$, will reach the point $\boldsymbol{x}$ at the time instant t_{n+1}.

$\boldsymbol{X}(\boldsymbol{x},t_{n+1};t)$ is the solution of initial value problem $\frac{d\boldsymbol{X}(\boldsymbol{x},t_{n+1};t)}{dt} = x$.

After calculation and simplification about (4), the floating process model now is simply affected by the ocean current velocity $L(t')$ and wind speed $u_W(t')$:

$$x(t) - x_0 = \int_0^t V(t')dt' = \int_0^t [L(t') + u_W(t')]\,dt'$$

(4.3.1.5)

In the floating model, we have simplified the floating object as a single particle, whose motivation obeys a certain distribution law and the motivation is independent. So the statistical area after floating for a certain time is the probability area of the floating object. We further assume the floating process is discrete and is a Markov Chain, which means the future state of the floating object only depends on its current state of forces and is irrelevant to its previous states [9], that is to say:

$$p(x_{i+1}|x_i, x_{i-1}, x_{i-2}, \dots x_1) = p(x_{i+1}|x_i)$$

(4.3.1.6)

According to (5) and (6), we obtain the stochastic floating process equation:

$$dx = V(x,t)dt + d\varepsilon$$

where x is the location of the object during the floating process; V is the velocity function of the floating object under forces; $d\varepsilon$ is the disturbance term which has a mean of zero ($\mathrm{E}(d\varepsilon) = 0$) and represents the character of the floating object and the uncertainty of forces. As the disturbance caused by water is relatively small, we only consider the disturbance caused by wind.

Many researchers [8,11] have concluded that the wind velocity obeys logarithmic normal distribution.

$$f(y) = \frac{1}{\sqrt{2\pi\sigma}y} e^{-\frac{(\ln y - \mu)^2}{2\sigma^2}}$$

$$y > 0, \sigma > 0, -\infty < \mu < +\infty$$

μ is the average number of wind velocity and σ is its standard deviation. We can determine these values from calculating statistical value of wind in a certain area during a certain period of time or refer to local meteorology record.

The integration time t_0 means the time from the aircraft crashed on ocean surface till rescue team arrived and set up the buoy.

With the help of Matlab, we can get the maximum possible value of floating radius R_m and locate possible search and rescue area.

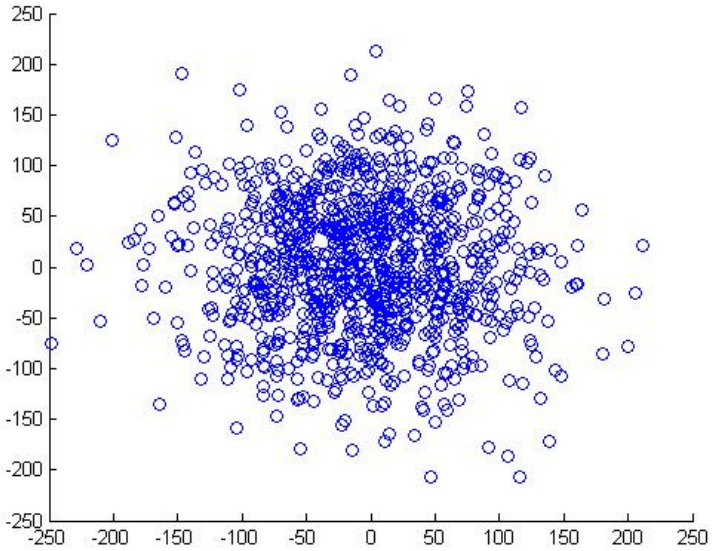


Fig. 4.3.1 Matlab simulation of the position of 1000 nodes using Monte Carlo method

4.3.2 Sinking Process

Wreckages of plane can be divided into two sorts by their density. Some has a low density and floats on the water, such as aviation fuel. The floating process model successfully studies the maximum floating distance. However, other parts of the wreckage have relatively high density, such as fuselage and black box, sinking to the bottom of the sea. The former floating model cannot be applied to sinking process. Thus, based on some reasonable assumptions, a new model has to be built.

Assume the ocean current as a Couette flow. It is an idealized situation where the water is assumed to be trapped between two horizontal plates, one fixed (the bottom of the sea) and one moving horizontally at a constant speed ***u*** (the sea level). Assume the fluid particles will move parallel to ***u***, and their speed will vary linearly from zero at the bottom to ***u*** at the top. Each layer of fluid will move faster than the one just below it, and friction (stem from dynamic viscosity) between them will give rise to a force resisting their relative motion.

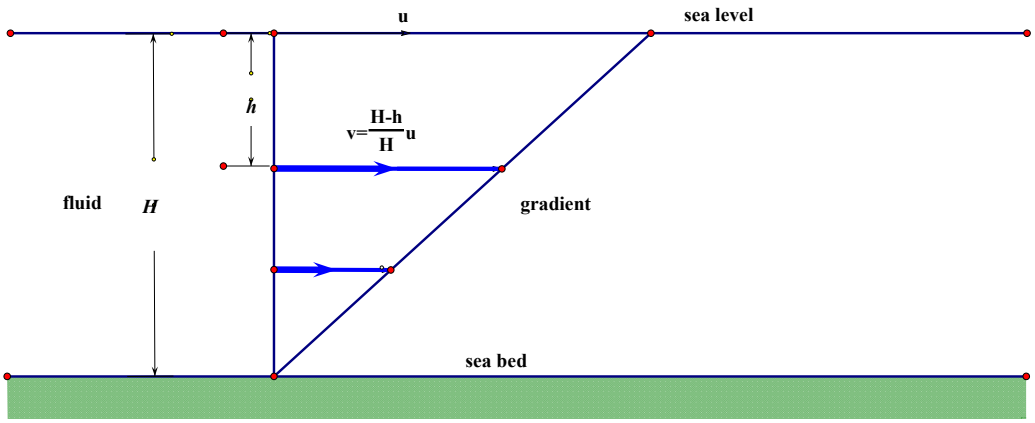


Fig.4.3.1 Ocean current under sea level

Assume wreckage receives water horizontal speed at once (ignore the process where object is driven by friction) within sinking process. Besides, Assume the wreckage has a constant vertical speed $\boldsymbol{u_{0\perp}}$ and has a zero horizontal speed. Assume wreckage becomes still at the moment it touches seabed (without rebound or embed). Denote the vertical friction between itself and the water as $f_\perp$, which is proportional to the varying $\boldsymbol{u}_\perp$ (wreckage vertical speed). Let the equation $f_\perp = ku_\perp$ describe the relationship. Apparently, $\boldsymbol{u}_\perp$ is a function of time *t*. Buoyancy ***B*** can be regarded as a constant (from Archimedes' principle). Hence, we get the following equation from Newton's second law:

$$m\dot{\boldsymbol{u}}_\perp = m\boldsymbol{g} - \boldsymbol{B} - k\boldsymbol{u}_\perp$$

(4.3.2.1)

Let **F** represent the constant force $m\boldsymbol{g} - \boldsymbol{B}$. Let k_0 represents the constant $\frac{k}{m}$. We get a differential equation

$$\dot{\boldsymbol{u}}_\perp + k_0\boldsymbol{u}_\perp = {\mathbf{F}}/{m}$$

On both sides, we times $e^{k_0 t}$. Now we get

$$\frac{\mathrm{d}\left(e^{k_0 t}\boldsymbol{u}_\perp\right)}{\mathrm{d}t} = {\mathbf{F}}/{m} \cdot e^{k_0 t}$$

Integral both sides, we get

$$\boldsymbol{u}_\perp = {\mathbf{F}}/{(mk_0)} + \boldsymbol{c}e^{-k_0 t}$$

Where c is a constant determined by the initial condition $\boldsymbol{u}_\perp(0) = \boldsymbol{u_{0\perp}}$

$$\boldsymbol{c} = \boldsymbol{u_{0\perp}} - {\mathbf{F}}/{(mk_0)}$$

Denote the depth of the ocean as *H*. We integral $\boldsymbol{u}_\perp$ from 0 to **T** (the time wreckage touches the bottom of sea).

$$\int_0^{\mathbf{T}} \boldsymbol{u}_\perp(\mathrm{t})\mathrm{dt} = {\mathbf{F}}/{(mk_0)} \cdot \mathbf{T} + \int_0^{\mathbf{T}} \boldsymbol{c}e^{-k_0 t}\mathrm{dt}$$

(4.3.2.2)

The left side equals to *H*. Hence we get the equation:

$$H - \frac{1}{k_0} = -\frac{1}{k_0}\mathrm{e}^{-k_0\mathbf{T}} + {\mathbf{F}}/{(mk_0)} \cdot \mathbf{T}$$

(4.3.2.3)

The solution of equation (4.3.2.3) gives the sinking duration **T**.

Now we calculate the horizontal displacement of the wreckage. After observation of the figure 4.3.1, the flow horizontal speed **v** is a function of **h** (the depth of wreckage). The geometric relationship is shown in the following equation

$$\frac{\mathbf{v}}{\boldsymbol{u}} = \frac{H - \mathbf{h}}{H}$$

As is calculated in (4.3.2.2), the value of **h** is given by the following equation

$$\mathbf{h}(\mathrm{t}) = {\mathbf{F}}/{(mk_0)} \cdot \mathrm{t} + \int_0^{\mathrm{t}} \boldsymbol{c}\mathrm{e}^{-k_0 s}\mathrm{ds}$$

(4.3.2.4)

Thus we have **v** in form of t.

We consider at time t, and in a short time dt, the velocity remains constant. That is to say, the wreckage sails a distance of $\mathrm{ds} = \mathbf{v}(\mathbf{t})\mathrm{dt}$. We simply integral ds from 0 to **T** to get the horizontal displacement s.

$$\mathrm{s} = \int_0^{\mathbf{T}} \frac{H - \mathbf{h}(\mathrm{t})}{H}\boldsymbol{u}\mathrm{dt}$$

where $\mathbf{h}(\mathrm{t})$ is given by equation (4.3.2.4)

The horizontal displacement assists the rescuers to determine the probable location in the seabed where wreckage sinks.

4.4 Model 4--- Search pattern

Since we have calculated a possible search area, the sector search pattern and expanding square search pattern are relatively effective compared with others listed in 1.2.2 when determining an appropriate search plan.

Buoys with GPS set as the datum-mark eliminate the effect of further disturbance caused from wind or water, enabling rescue team to follow a specific pattern accurately.

4.4.1 Model of radar or sonar system

The available scan area of a radar or sonar system equipped on a rescue plane is a cone with a top angle of 2α. Here, we note that different types of search planes have different types of electronics and sensors, which probably means the top angle 2α can vary. When the plane is flying straight forward at the height of H, the cross section of the search area is a triangle with base length of $Htan(\alpha)$ and height of H.

As a rescue plane may not possibly find all the target in its search area, we define an expected rate of p to estimate the possibility of finding the target.

To simplify calculation, we assume that the target can only be found when the cross section of the cone reaches it.

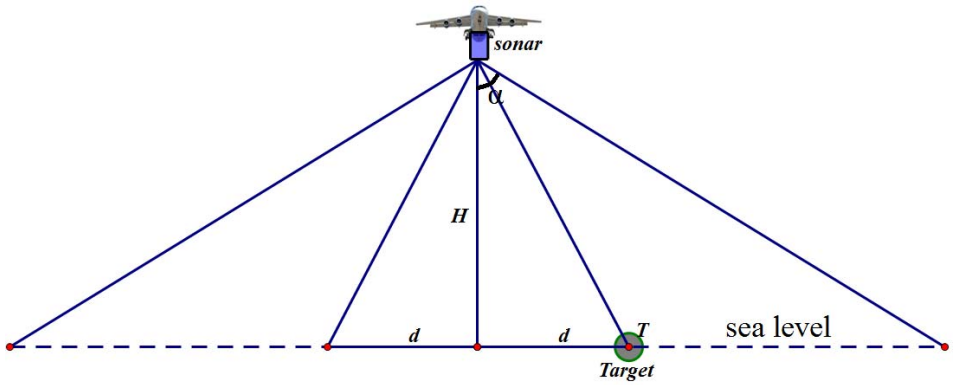


Fig 4.4.1.1 Searching floating target

The distance of the target (T) to the point directly below of the search plane (B) is s. The expected rate is defined as

$$p(s) = \begin{cases} 1 - \dfrac{\arctan(\frac{s}{H})}{\alpha}, & 0 \le s < Htan(\alpha) \\ 0 \quad , & s \ge Htan(\alpha) \end{cases}$$

4.4.2 Sector search pattern

According to the sector search pattern, a search plane turns to the right of 120 degree when it reaches the edge of possible search and rescue area. So the search area is divided into six sector with 60 degree center angle. Three planes can search along the edge of three noncontiguous sectors at the same time if there are enough searching planes.

A target may be scanned by a search plane for 2 or 3 times in the same sector.

When target location is in Fig 4.4.2.1, only routes $r1, r2, r3$ are supposed to be able to find the target because of their relatively shorter distance. When target location is in Fig 4.4.2.2, only routes $r1, r4$ are supposed to be able to find the target. Other situations are similar. θ is marked in figure to show its angle.

The rough total expectation of target ($0 \le \theta \le \frac{2\pi}{3}$) being found is

$$PS = \sum_i p_i(s)$$

$$= \begin{cases} 3 - f\left(\frac{\arctan\left(\frac{y}{H}\right)}{\alpha}\right) - f\left(\frac{\arctan\left(\frac{\sqrt{x^2+y^2}}{H}\right)}{\alpha}\right) - f\left(\frac{\arctan\left(\frac{|\sqrt{3}(x-R_m)+y|}{2H}\right)}{\alpha}\right), 0 \le \theta \le \frac{\pi}{3} \\ 2 - f\left(\frac{\arctan\left(\frac{|\sqrt{3}x-y|}{2H}\right)}{\alpha}\right) - f\left(\frac{\arctan\left(\frac{|\sqrt{3}x-y|}{2H}\right)}{\alpha}\right), \frac{\pi}{3} < \theta \le \frac{2\pi}{3} \end{cases}$$

$$f(x) = \begin{cases} 1, & x < 0 \\ x, & x \ge 0 \end{cases}$$

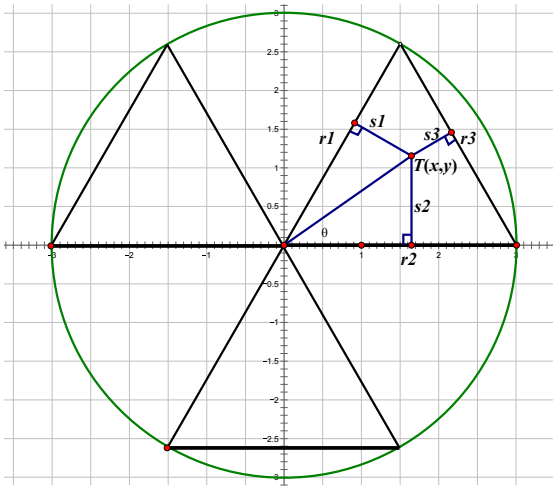


Fig 4.4.2.1

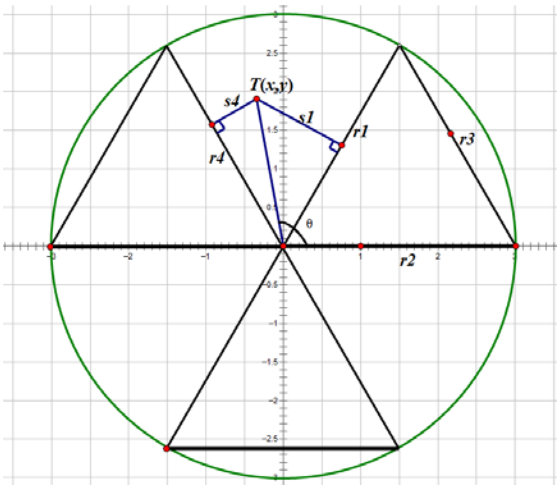


Fig 4.4.2.2

Two kinds of target locations

Flight height of search plane H and top angle α are certain numbers, so there exists a R_m when sector search pattern covers all searching circle, otherwise, some less important area is neglected.

$$R \le \begin{cases} 2\sqrt{3}Htan(\alpha), & 0 \le \theta \le \frac{\pi}{3} \\ \frac{4\sqrt{3}}{3}Htan(\alpha), & \frac{\pi}{3} < \theta \le \frac{2\pi}{3} \end{cases}$$

R is different towards two parts of θ, Fig 4.4.2.3 illustrates the situation when R exactly fills the sector $0 \le \theta \le \frac{\pi}{3}$. All the search circle area can be covered when R satisfies:

$$R \le \frac{4\sqrt{3}}{3}Htan(\alpha)$$

(4.4.2)

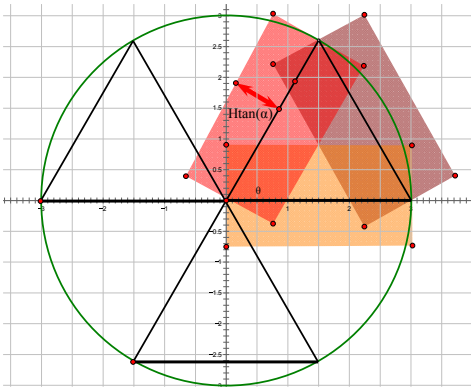


Fig 4.4.2.3 The situation when R exactly fills the sector

When target T is in sector $\frac{2\pi}{3} < \theta \leq 2\pi$, it is similar as there is strong symmetry in this pattern.

4.4.3 Expanding square search pattern

The flight route of expanding square search pattern is shown below. We set the gap between two routes as $Htan(\alpha)$, which means a target may be scanned 2 or 3 times (assuming scan stops when turning direction at corners). Search area of one part of route is painted purple in Fig 4.4.3.1. When the target is located in A square (marked in Fig 4.4.3.1), it is scanned for 3 times, and 2 times in other situations.

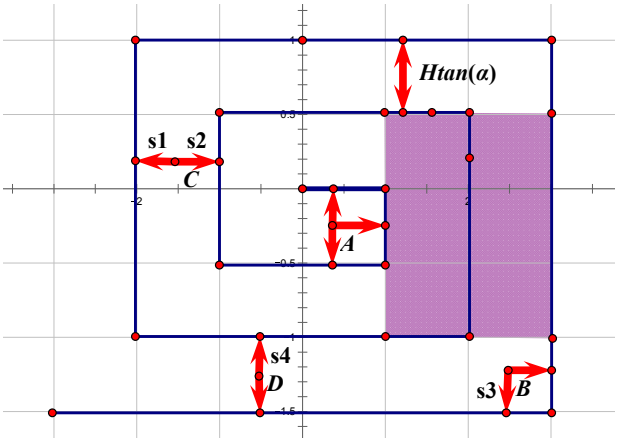


Fig 4.4.3.1 route of expanding square search pattern

$s1, s2, s3, s4$ are four directions towards the target. Their possibility of being found $p(s)$ is

When $s1$ is horizontally outward

$$p(s1) = 1 - f\left(\frac{\arctan\left(\frac{Htan(\alpha) - Rem(|x|, Htan(\alpha))}{2H}\right)}{\alpha}\right)$$

When $s2$ is horizontally inward

$$p(s2) = 1 - f\left(\frac{\arctan\left(\frac{Rem(|x|, Htan(\alpha))}{2H}\right)}{\alpha}\right)$$

When $s3$ is vertically outward

$$p(s3) = 1 - f\left(\frac{\arctan\left(\frac{Htan(\alpha) - Rem(|y|, Htan(\alpha))}{2H}\right)}{\alpha}\right)$$

When $s4$ is vertically inward

$$p(s4) = 1 - f\left(\frac{\arctan\left(\frac{Rem(|y|, Htan(\alpha))}{2H}\right)}{\alpha}\right)$$

$Rem(a, b)$ is the remainder after division a/b.

With the combination result of $p(s)$, we can get PS of every situation.

$$PS = \sum_i p_i(s), i = 2 \; or \; 3$$

4.4.4 Estimate effectiveness and efficiency

The difference between two search route patterns determines the effectiveness and efficiency of search. The sector search pattern searches the center area more often, which is the area with relatively high probability. It saves search distance and time, but may neglect certain part of area when R_m cannot meet the requirement of (4.4.2). Expanding square search pattern searches from the center to the periphery with no neglect, which takes relatively low efficiency, but has steady possibility to find the target.

When we determine an appropriate search pattern, we design an index to compute efficiency and effectiveness to balance the pros and cons of the search pattern. We define the effectiveness per time as follows.

Expectation time of finding the target is defined as

$$TS = \sum_{i=1}^{N} p_i(s) t_i = \sum_{i=1}^{N} \prod_{j=1}^{i-1} [1 - p(s_j)]\, p(s_i) \frac{r_i}{v}$$

N is the total number of possible routes searching for the target, t_i is the flight time to find target on route i, r_i is the flight distance to find target on route i, v is the speed of the search plane.

Define $l(x, y)$ as the possibility of target falling to the point (x, y).

Expectation of the possibility of finding the target per time is defined as

$$E = \iint l(x, y) \frac{p_i(s)}{t_i}$$

4.4.5 Comparison between two search patterns

The average wind speed is 8 m/s and variance is 2 $(m/s)^2$ in South Indian Ocean in March [12]. The flight height of search plane H is 300 to 600 meters [3]. Top angle α varies according to the searching devices. Here we let $\alpha = \frac{\pi}{3}$. t_0 is the time from the aircraft crashed on ocean surface till rescue team arrived and set up the buoy, which varies from cases. Here we choose 1.5 hours in the simulation.

Determining the variance of wind velocity σ is quite difficult, as the velocity difference between two very short time is difficult to obtain. But we find that σ has little impact towards E and R_m when it is less than 0.1. We use constant value 0.01 in the future simulation.

	t_0(s)	μ(m/s)	σ^2(m^2/s^2)	H(m)	α(rad)
Chosen values	5400	8	2	500	$\frac{\pi}{3}$

Table 4.4.5.1: Values we choose in simulation

As all the values have been chosen, we can calculate indexes E, TS, PS and R_m using two searching patterns.

t_0 is a sensitive variable in this model, as it is quite uncertain for the search team to arrive at the crash spot, so we further investigate the impact of t_0 on these indexes and offer a relatively sensible search pattern for rescue team to search.

When t_0 is small, the wreckage will not float a long distance, causing a dense distribution in the center of the crash point, which has higher possibility for sector search pattern to find the target, but the expanding square search pattern has relatively low influence towards center area, moving to one direction at the center point, leaving about half of all points near center area behind, resulting its low PS.

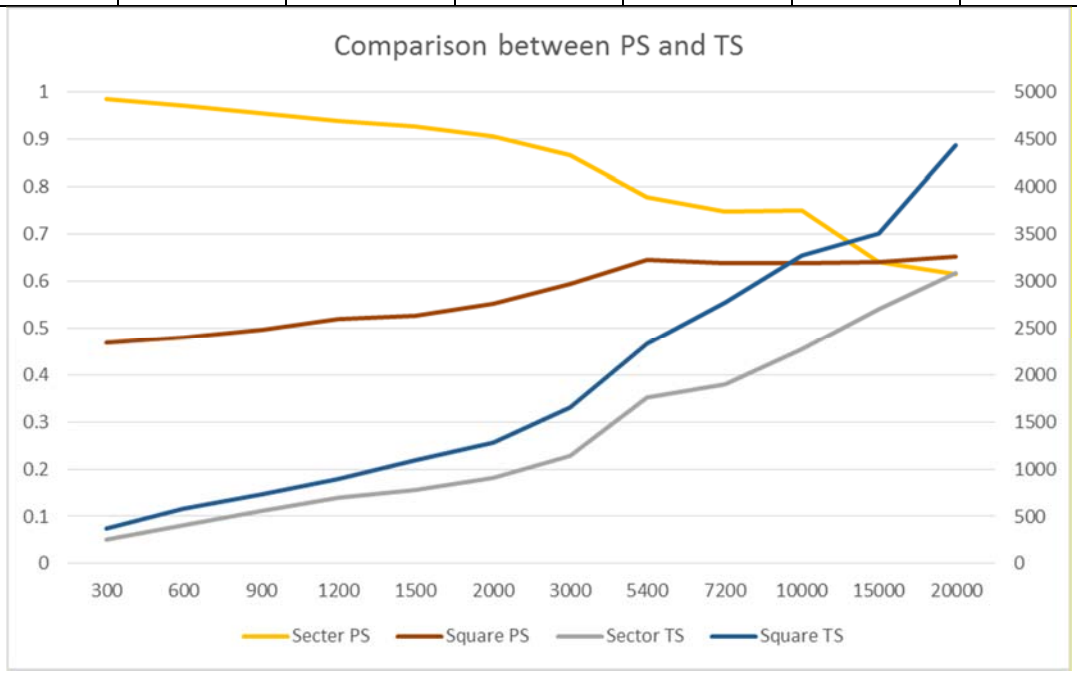
However, when t_0 is getting larger, such as after 1.5 hours, the floating process has been obvious, the maximum floating distance is over one nautical mile(1852m). According to (4.2.2), the sector search pattern begins unable to cover the full search area. So after that time point, PS begins to drop dramatically. When more points spread widely, PS of expanding square search pattern rises gently. Around $t_0 = 15000(s)$, PS of expanding square search pattern is larger.

At the same time, R_m gets larger with t_0, resulting a longer time TS to finish the search and E between these two patterns are largely reduced.

With the analysis of all these indexes, we can conclude that, when t_0 is within a given balance point, using sector search pattern can find float target with more possibilities and less time, which is much more effective and efficient than expanding square search pattern. However, the sector search pattern could be ineffective when t_0 is beyond a certain point, in which case may result in large possibility of not finding the target with huge amount of time.

We draw the chart and table comparing between sector search pattern (Sector) expanding square search pattern (Square) in Table and Fig 4.4.5.1.

t_0	300	900	1500	3000	5400	7200
Sector E	9.98E-03	5.20E-03	3.99E-03	2.79E-03	1.50E-03	1.50E-03
Sector Rm	4.49E+02	7.81E+02	1.01E+03	1.43E+03	1.99E+03	2.18E+03
Sector TS	2.55E+02	5.53E+02	7.84E+02	1.14E+03	1.75E+03	1.89E+03
Sector PS	9.86E-01	9.54E-01	9.27E-01	8.68E-01	7.77E-01	7.47E-01
Square E	1.72E-02	8.02E-03	5.06E-03	3.42E-03	1.76E-03	1.63E-03
Square Rm	4.69E+02	7.81E+02	1.00E+03	1.42E+03	1.88E+03	2.13E+03



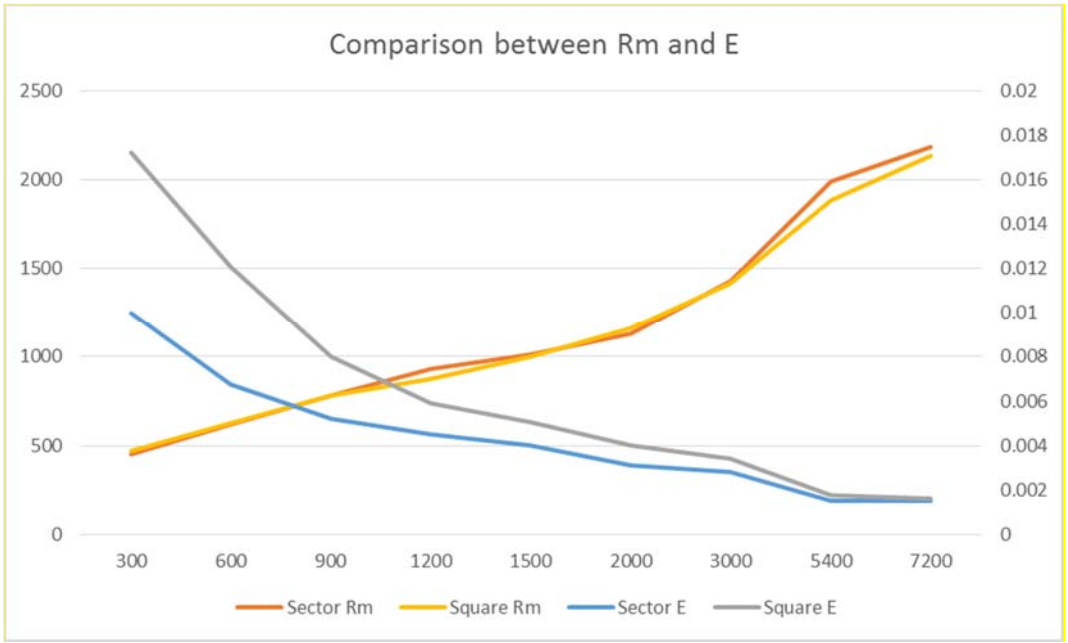


Table and Fig 4.4.5.1 Trend of PS, TS, E and R_m with increasing t_0 between Sector search pattern(Sector) and Expanding square search pattern(Square)

5. Verifications of our model

5.1 Verification of Model 1

Since the location where MH370 lost contact has not been officially determined, we use official data of Air France Flight 447 to verify the effectiveness of this model [11].

Air France Flight 447 was a scheduled passenger flight from Rio de Janeiro ($22°\mathrm{S}, 43°\mathrm{W}$), Brazil to Paris ($49°\mathrm{W}, 2°\mathrm{E}$), France, which crashed on 1st June 2009. The aircraft departed on 31 May 2009 at 22:29 UTC the last verbal contact with the aircraft was at 01:35 UTC, 3 hours and 6 minutes after the 22:39 UTC departure.

The Airbus 330, involved in the accident, takes approximately 15 minutes to reach the cruise speed, about 0.82 Mach (1004 km/h). We assume the accelerating process as a uniformly accelerated motion. Denote the accelerating distance (begins with zero speed and ends up with the cruise speed v_c) s_0. The following equation gives the value of s_0.

$$s_0 = {at^2}/{2}$$

Where $a = {(v_c - 0)}/{t} = \frac{1004}{0.25} = 4016 km/h^2$, t=0.25h

Hence we have s_0=125.5 km. The plane is cruising at a constant speed v_c during the remaining 2.75 hours.

Denote the cruising distance before crash as s_c. The cruising distance can be regarded as a uniform motion. Hence, $s_c = v_c t$=1004*2.75=2761 km.

Hence the total s=$s_0 + s_c$=2886 km. The earth radius is 6371 km.

In equations (4.1.2), Let p_1=43°, q_1=−22°, $p_2 = -2°$, $q_2 = 48°$.

With the assistance of Matlab, we get the coordinate of P (falling point). The results turns out to be (5467.8, 3267.7, 124.1). Converse it into longitude-latitude form. We get (30.9°W, 1.1°N).

According to the final report issued by BEA (Bureau d'Enquêtes et d'Analyses), the site of accident is 3°03’57’’ N, 30°33’42’’ W. Compared to the calculated result 1.1°N, 30.9°W, considering reasonable approximation, it strongly proves the effectiveness of Model 1.

5.2 Verification of Model 2

We still use official data of Air France Flight 447 to verify Model 2.

First, we make two reasonable assumptions:

(1) When the plane fell down, it was flying at cruise speed v_c.

(2) The direction angles of initial velocity v_0 (α, β, γ) equals $(\alpha, 0, \frac{\pi}{2} - \alpha)$, which is a reasonable assumption after observation of figure above.

According to the analysis in Model 2, $v_0 = \sqrt[2]{{v_c}^2 + 2g\mathrm{h}}$, $\tan\alpha = \frac{\sqrt{2gh_c}}{v_c}$. Where $h_c = 10000m$ (cruise height) and v_c=1004km/h (cruise speed), all the data from A330 official standard.

λ is the latitude of accident site. From the BFA report, λ equals to $33°03'$.

Given all the values above, with the assistance of Matlab, we solve the equation (4.2.5) z=0. After getting the t value, we work out the coordinate of plunging point (x, y, z).

BFA published the sonar images of possible plunging points. We check Fig 5.2 to get the longitude and latitude. The results match the image well.

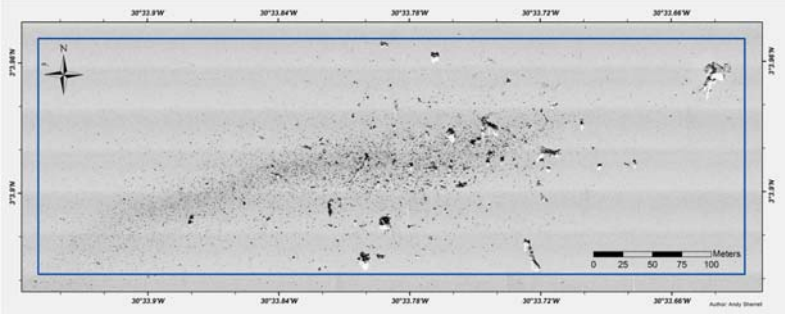


Fig 5.2 Sonar images of possible plunging points for Air France Flight 447

The Air France Flight 447 case sustainable supports the effectiveness of Model 2.

6. Sensitivity Analysis

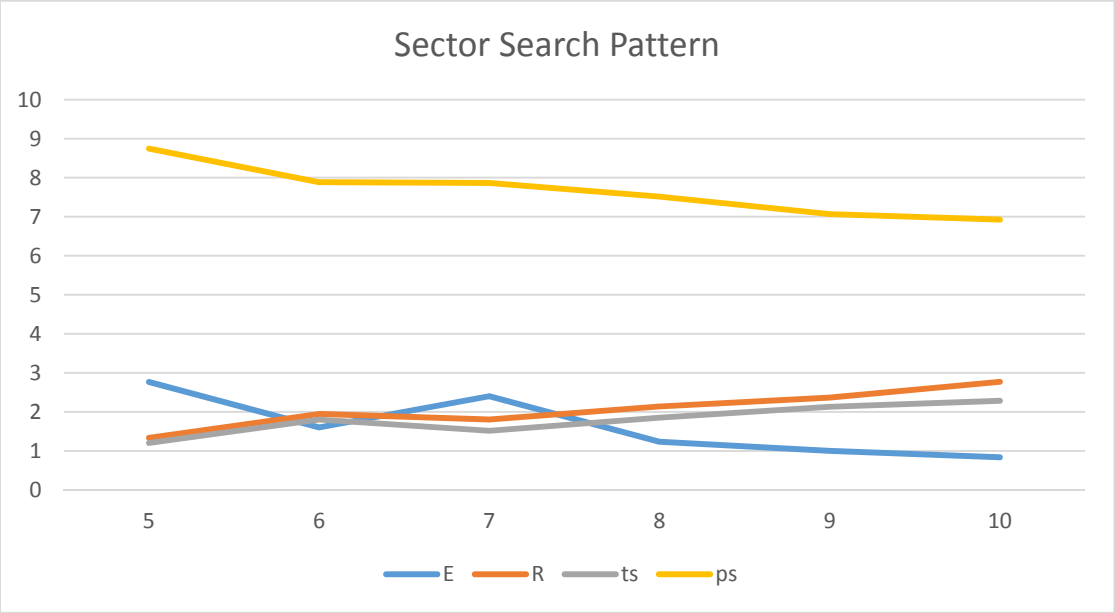
In model 4, we design several indexes to describe the effectiveness and efficiency of search patterns. Apparently, these indexes (E, TS, PS, R_m) are functions of wind velocity. As is clarified in Model 4, we simply let wind velocity be 8 m/s (mean value of spring wind velocity in Indian Ocean). However, in order to build a generic model that is applicable in other part of the world, we need to analyze the effect of wind velocity on these indexes.

In order to eliminate the great uncertainty and significant variances, for each wind velocity, we calculate these four indexes 10 times and take the average as the final values.

The results are shown in the following table.

Table 6.1: Sector Search Pattern

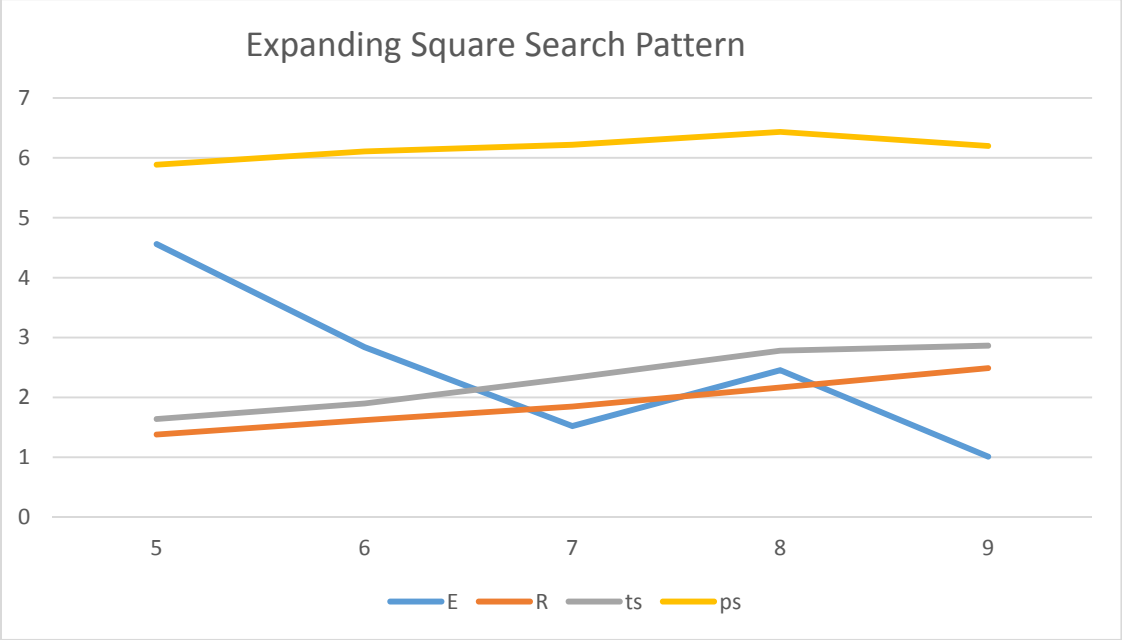
Wind Velocity(m/s)	E(1/s)	R_m(m)	TS	PS
5	0. 002766	1333. 422	1202. 725	0. 874465
6	0. 001603	1944. 129	1801. 759	0. 788191
7	0. 0024	1802. 431	1514. 144	0. 78618
8	0. 001232	2139. 621	1850. 519	0. 751212
9	0. 000999	2364. 374	2130. 632	0. 706531
10	0. 000835	2770. 157	2281. 587	0. 69231



(6.1)

Table 6.2: Expanding square search pattern

Wind Velocity(m/s)	E(1/s)	R_m(m)	TS	PS
5	0.00456	1379.138	1637.625	0.58859
6	0.00284	1619.988	1897.175	0.61074
7	0.00152	1848.038	2325.213	0.62164
8	0.002454	2164.836	2779.819	0.643334
9	0.00101	2488.313	2863.4	0.6199
10	0.001	2802.088	3083.35	0.5903



(6.2)

Some conclusions can be easily observed from the above figures:

(1) E is approximately a monotone decreasing function of wind velocity.

No matter which search plan we choose, with the expansion (stem from increasing wind velocity) of search area, the effectiveness and efficiency decrease greatly).

(2) TS and R_m are monotone increasing function of wind velocity.

Increase in R_m reflects the expansion of the search area, which is a direct consequence of increasing wind velocity. With the expansion of the search area, both of the plans show longer expected searching time.

(3) As for Sector Search Pattern, PS is a monotone decreasing function, while it is a monotone increasing function for Expanding Square Search Pattern.

The reason for the difference is almost the same as the analysis in Model 4. Actually, wind velocity here, exerts similar influences on the model compare to t_0. Thus, the index curves above show similar properties compared to Figure 4.4.5.1.

To analyze the sensibility of parameter wind velocity, we calculated the indexes when wind velocity equals 7.6 and 8.4 (5% deviated from 8). The results are shown in the following tables.

Table 6.3: Sector Search Pattern

Wind velocity (m/s)	7.6	8	8.4	Mean Percentage deviated from 8
E(1/s)	0.001234	0.001216	0.001318	4.93%
R_m(m)	2281.252	2228.025	2428.606	5.70%
TS	2021.145	1929.505	1958.645	3.13%
PS	0.766186	0.746397	0.731824	0.349%

Table 6.4: Expanding Square Search Pattern

Wind velocity (m/s)	7.6	8	8.4	Mean Percentage deviated from 8
E(1/s)	0.001796	0.001443	0.001218	20.03%
R_m(m)	1983.226	2177.077	2312.129	7.55%
TS	2695.211	2661.663	2840.283	3.99%
PS	0.649599	0.650805	0.637398	1.13%

From these two tables, as for Sector Search Pattern, all four indexes are not sensitive to wind velocity change. However, for Expanding Square Search Pattern, E is highly sensitive to wind velocity change. Thus, Expanding Square Search Pattern is lack of stability.

7. Weaknesses and Strengths of the Model

Model 1:

Strengths:

- Our model is objective and conforms to reality, for we have selected the great circle courses as airlines. Generally rhumb lines are easier for coordinates transformation and calculation, but planes always fly along the great circle courses.
- The mathematical model we construct here is simple to understand with a small amount of mathematical skill. And, the calculation of it can be solved by simple mathematical software such as Matlab.

Weaknesses:

- In order to create a calculable model, we have assumed that the planes wouldn't deviate from the present courses, which is not realistic.
- We have not considered the impact of Coriolis force on the flying planes.

Model 2:

Strengths:

- We take Coriolis force and air resistance into consideration when creating the generic projectile motion model, which is more approximate to the actual condition.

Weaknesses:

- In order to simplify calculation, when using Conservation of Energy Theorem to figure out v_0, we ignore the impact of Coriolis force and drag force on planes.
- When calculating t in this model, we simply let *z*=0 be the plunging condition to simplify the problem. However, the horizontal displacement does exist, so the result is not exactly accurate.

- We have regarded the direction of v parallel to the ground at the highest to simplify calculation, which may not be objective and realistic.

Model 3:

Strengths:

- We consider both high-density wreckage and low-density wreckage. Respectively build floating and sinking model to study these two processes.
- With the assistance of FVCOM and reformulated Navier-Stokes model, which are regarded as the most useful methods, we study how the ocean current affects the motion of wreckage. When dealing with the sinking process, we attentively study the vertical and horizontal motion. Finally, we accurately give the maximum horizontal range for searching.
- In this model, we use data and quantitative analysis as foundations, and all the data we adopt is developed by reliable databases, so the output is objective and reasonable.

Weaknesses:

- Application of Monte Carlo method needs a large amount of samples and calculation. However, given the limited equipment and time, 10000 samples has already exerted great pressure on the computer. Thus, the calculation result of Model 3 varies to some extent and contains uncertainty.

Model 4:

Strengths:

- We have selected the most common search patterns in reality and studied the efficiency and effectiveness through well-designed algorithm. Well-defined index E has been applied to compare and judge different search patterns.
- More importantly, the algorithm and index in this model is generic and apply to every possible search pattern theoretically (Consider that different types of search planes have different top angles when transmitting search signals).

Weaknesses:

- Similar to Model 3, the application of Monte Carlo method to determine probability distribution of wreckage location brings about uncertainty and fluctuation. Besides, lack of sustainable data makes the estimation of flight height of search planes and technical standards of sonars difficult.

8. References

[1] Chris Ashton, Alan Shuster Bruce, Gary Colledge and Mark Dickinson (2015) The Search for MH370. *The Journal of Navigation* 68 (01), pp. 1-22

[2] Xu yanjiang (2012) Ways of Determining Search and Rescue Area at Sea [D] (In Chinese)

[3] Chen mingdong (2007) Research on Maritime Searching Techniques [D] (In Chinese)

[4] Zhou Qihuan, Lu xuejun, (1997) An Introduction of FANS Route and the Measuring Method Of the Shortest Route. Aviation Economics and Technology, No. 188 (In Chinese)

[5] Liu guangsheng (2010) Numerical Simulation of the Effect of River on Near-shore Hydrodynamics using Unstructured Grid Model [D] (In Chinese)

[6] Marı´a Luisa Co´rdoba, Antonio Garcı´a Dopico, M Isabel Garcı´a, Francisco Rosales, Jesu´s Arnaiz, Rodolfo Bermejo and Pedro Gala´n del Sastre (2014) Efficient Parallelization of a Regional Ocean Model for the Western Mediterranean Sea. *The International Journal of High Performance Computing Applications* Vol. 28 (3) 368-383

[7] Jiang hualin (2011) Study on Determining Search Area Model for SAR at Sea [D] (In Chinese)

[8] Zhou Zhengqiang, (1987) Calculation of annual maximum wind speed using logarithmic normal distribution. *Meteorology* Vol. 13, No. 12 (In Chinese)

[9] Jiang hualin, Sun zhaochen, Li li, Liu bo, Wu junping (2011) Determining maritime search area model based on Monte Carlo method. *Journal of Waterway and Harbor* Vol. 32, No. 4 (In Chinese)

[10] Wang anxiang, Zhang xiaojun, Zhai xuejun and Chang hongfang (2012) Research on a Remote Projectile Considering the Air Resistance and the Earth Rotation. *Mechanics in Engineering [J]* 34 (4) (In Chinese)

[11] MENG Qingzhen, DU Jian,(2001) Comparison of fitting results of four distribution functions to asymptotic distribution of yearly maximum surface wind speed over Chengdu. Journal of Chengdu University of information technology Vol. 16, No. 2 (In Chinese)

[12] Xu Guolong, (2012) Indian Ocean sea surface wind field temporal distribution characteristics and trend analysis. Hydrometeorological, geological disasters and weather forecast service[C].

[13] BEA Bureau d'Enquêtes et d'Analyses pour la sécurité de l'aviation civile (2012) Final Report On the accident on 1st June 2009 to the Airbus A330-203 registered F-GZCP operated by Air France flight AF 447 Rio de Janeiro – Paris

[14] Wang jian, Han xiulin (2009) Movement of Projectile Affected by the Resistance of Air and the Rotation of the Earth. *Journal of Anqing Teachers College (Natural Science Edition)* Vol. 15, No. 4 (In Chinese)

[15] A. GARCIA, J.L. TORRES, E. PRIETO and A. DE FRANCISCO (1998) Fitting Wind Speed Distributions: A Case Study. *Solar Energy* [J] Vol. 62, No. 2, pp. 139–144

[16] Roy Streit (2014) Real-time Wind Speed Estimation and Compensation for Improved Flight. *IEEE transactions on aerospace and electronic systems* Vol. 50, No. 2

[17] Øyvind Breivik, Arthur A. Allen (2008) An Operational Search and Rescue Model for the Norwegian Sea and the North Sea. *Journal of Marine Systems* 69, 99-113

[18]Paul S. Epstein (1931) On the Air Resistance of Projectiles. *Physics* [J] Vol. 17, 532-547

[19] W. Ferrel (1858) The Influence of the Earth's Rotation upon the Relative Motion of Bodies near Its Surface. *The Astronomical Journal* No. 109, 97-100

[20] Liu guangqiang (2009) Research on Determining Sweep Widths for Sea Searches [D] (In Chinese)

[21] Qiu ping (2006) Study on Best Search Area and Search Methods [D] (In Chinese)

[22] Xia liang, Wu zhendong (2002) Study on Helicopter Search and Rescue Methods. *National Helicopter Annual Meeting Papers* [C] (In Chinese)

9. Appendix (Non-technical Paper)

MEDIA STATEMENT BY ABC AIRLINES

Good morning ladies and gentlemen, members of the media.

I am here today on behalf of the director of Technology Department of ABC Airlines.

As you are aware, air crashes frequently take place in recent years. It has been a frustrating time for most of us. Life is precious to every one of us, so ABC Airlines takes offering the safest flights to passengers as our mission. Nevertheless, in case of unexpected mishaps, we as well commit to spare no efforts to search and rescue our sibs.

Today I'm on behalf of ABC Airlines here to demonstrate two effective future search plans based on the generic mathematical model we've built to assist "searchers" in planning a useful search for a lost plane feared to have crashed in open water.

Our search plans consider both floating and sinking processes of low-density and high-density aircraft wreckages. Better still, ocean current and wind velocity have been analyzed in the two search plans to better locate the wreckage position. In reality, the probability of wreckage location doesn't obey the uniform distribution. However, the probability distribution is uniform along most of the actual search routes of search planes. So our future search plans have selected sector and expanding square search patterns.

Sector search patterns are adopted in the first search plan. In this plan, we denote LKP as the intersection of the three congruent triangles. Three search planes start to fly along three different sides of three triangles at the same time. The length of the side is determined as search radius, and the center is LKP. Search planes would turn to the right of 120 degree when they reach the edge of possible search and rescue area. A target may be scanned by a

search plane for 2 or 3 times in the same search period, which to some extent may improve the accuracy of possibility of being found.

Expanding square search patterns are adopted in the second plan. In this plan, we as well denote LKP as the starting point of the route along expanding square. The gap between two routes hints that a target may be scanned 2 or 3 times (assuming scan stops when turning direction at corners), which indicates this plan of searching is more complete and effective rather than efficient.

Above two search plans demonstrate feasible and practical search routes when air crash unexpectedly takes place. Through Comparison, we get that when search target is located in a limited area, sector search pattern is effective. Buoys with GPS are used to set as the datum-mark. Expanding square search pattern searches from the datum-mark and expands search lines outward.

Generally speaking, our airlines have developed two effective future search plans based on the generic mathematical model we've built to assist "searchers" in planning a useful search for a lost plane. We sincerely hope every passenger a safe journey, and in case of unexpected air crash, we once again heartfelt hope the search plans offered can be of great help in reality.

Thanks ladies and gentlemen, members of the media!

ABC AIRLINES